Available online at www.sciencedirect.com
SCIENCE DIRECT®
Solid State Ionics 166 (2004) 157–165
SOLID STATE IONICS
www.elsevier.com/locate/ssi

Impedance spectroscopy analysis of percolation in (yttria-stabilized zirconia)-yttria ceramic composites

F.C. Fonseca*, R. Muccillo

Centro Multidisciplinar para o Desenvolvimento de Materiais Cerâmicos, CCTM-Instituto de Pesquisas Energéticas e Nucleares, C.P. 11049, Pinheiros, 05422-970-S. Paulo, SP, Brazil

Received 12 September 2003; received in revised form 12 September 2003; accepted 1 October 2003

Abstract

$(ZrO_2$:8 mol% $Y_2O_3)+m$ mol% Y_2O_3 ceramic composites with nominal yttria concentration varying from 0 to70 mol% (0–82.9 vol.%) were prepared by evaporation of a suspension of ZrO_2:8 mol% Y_2O_3 and Y_2O_3 in ethanol followed by pressing and sintering. The samples were analyzed by X-ray diffractometry and scanning electron microscopy for microstructural characterization. The electrical properties were studied by impedance spectroscopy (IS) allowing for the separation of the inter- and intragranular components of the electrical conductivity. The percolative behavior of these components was analyzed using the general effective media (GEM) equation and the percolation thresholds found were ~ 28 vol.%. The results indicate that impedance spectroscopy provides useful information in addition to the dc techniques concerning the electrical characterization of composite materials.

PACS: 84.37.+q; 81.05.Je; 72.80.Tm
Keywords: Impedance spectroscopy; Ceramic composites; Zirconia–yttria; Percolation

1. Introduction

Zirconia-based solid electrolytes are the major components of devices with different applications such as oxygen sensors, oxygen pumps and solid oxide fuel cells (SOFC). These devices take advantage of the oxide ion conduction of the zirconia-based solid electrolytes to monitor oxygen content in a gas mixture (sensor), generate controlled oxygen partial pressures (pump) and produce energy (SOFC). As a device component, yttria-stabilized zirconia (YSZ) is usually found connected to different materials or as a composite. For example, in SOFCs using YSZ as the electrolyte, the typical cathode and anode materials are the lanthanum–strontium manganites and the nickel/yttria-stabilized zirconia cermet, respectively [1,2]. Composite materials are suitable to improve or complement the electrical, chemical and structural properties of stabilized zirconia to get the maximum efficiency required on the different processes taking place in specific applications. Particularly, the electrical conduction properties of zirconia-based solid electrolytes are largely influenced by the presence of a dispersed second phase or impurities. As a consequence, systematic studies concerning the influence of impurities, and the role played by a disperse second insulating phase on bulk and grain boundary transport properties are necessary to better understand the transport mechanisms in zirconia-based solid electrolytes.

Concerning the electrical characterization of solid electrolytes, the impedance spectroscopy (IS) is frequently used to separate the different contributions to the electrical resistivity. The electrical response of polycrystalline YSZ in the electrolytic region, determined by IS in the Hz to MHz frequency region shows two semicircles in the impedance diagram [3]: one at high frequencies (HF) is characteristic of the bulk (intragranular) response; other, at low frequencies (LF) is related to the blocking of charge carriers due to the internal surfaces of the polycrystalline specimens, also denoted intergranular response [4–6]. Impedance diagrams of YSZ specimens with controlled additions of insulating second phases such as alumina [7], or microstructural defects such as pores [8], show a larger increase in the low frequency semicircle than in the high frequency one. That means that the main effect of adding insulating second

* Corresponding author. Tel.: +55-11-38169343; fax: +55-11-38169343.
E-mail addresses: cfonseca@ipen.br (F.C. Fonseca), muccillo@usp.br (R. Muccillo).

0167-2738/$ - see front matter © 2003 Elsevier B.V. All rights reserved.
doi:10.1016/j.ssi.2003.10.002

phases to zirconia solid electrolytes is to increase the electrical resistance of the internal surfaces of the electrolyte. The increase in the low frequency electrical resistance characterizes the blocking of charge carriers and depends on the amount of blockers.

Thus, the study of the electrical properties of composites of the type YSZ-insulator using IS can be useful to better understand the transport properties of zirconia-based materials. The study of the electrical properties of composites is motivated by both technological and scientific interests. The electrical properties of composite materials are usually determined by the specific electrical properties of each phase, the relative concentration, distribution and morphology of the components. The prediction of the electrical conduction of metal-insulator (MI) composites is an extensively studied subject and has been a research theme for decades but so far no analytical solution for real composite structures is found [9–11]. Various models try to correlate some of the most important variables like electrical conductivity, relative concentrations and morphology of individual phases [11]. In the case of solid electrolyte-insulator composites, interfacial interaction effects can generate space-charge regions near the phase boundaries with a concentration profile of ionic charge carriers. These systems have already been experimentally [12,13] and theoretically [14,15] investigated, and the main finding is an increase of the electrical conductivity of solid electrolytes with the addition of finely dispersed insulating second phase, resulting in a bell-shaped dependence of electrical conductivity with further insulator additions. In general, the effective media and percolation theories can be used for predicting physical properties, such as electrical resistivity, thermal conductivity, dielectric constant and magnetic susceptibility of composite media. Near to the percolation threshold a continuous path is formed through the specimen and an abrupt change of the transport properties is observed [16]. This critical behavior is related to the divergence of a characteristic correlation length that obeys a scaling law with parameters like the electrical conductivity, and depends only on the microstructure of the percolating cluster and on the ratio of electrical conductivities of the phases [17]. The real part of the electrical conductivity is a parameter usually used to the to study the percolation of MI composites and several experimental and theoretical works have been performed in the past decades [11,18].

The effective medium theory assumes that a particle (conducting or insulating) is surrounded by a mixture of the two components, which has the mean or effective value for the medium [19]. A general effective media (GEM) equation for the electrical resistivity of composites that combines percolation and effective medium theories was proposed by McLachlan [20,21]:

$$\frac{(1-f)\cdot\left(\rho_M^{1/t}-\rho_H^{1/t}\right)}{\rho_M^{1/t}+A\cdot\rho_H^{1/t}}+\frac{f\cdot\left(\rho_M^{1/t}-\rho_L^{1/t}\right)}{\rho_M^{1/t}+A\cdot\rho_L^{1/t}}=0 \qquad (1)$$

where ρ_M, ρ_H and ρ_L are the resistivities of the composite, of the high resistivity phase and of the low resistivity phase, respectively; t is a percolation critical exponent; f and f_C are the volume fraction and the critical (percolation) volume fraction of the low resistivity phase, respectively; and $A=(1-f_C)/f_C$. This equation has been successfully used to analyze the electrical properties of several different composite materials [11,22–24]. More recently, a new version of the GEM equation, which takes into account two critical exponents, in similarity with classical percolation equations, was also proposed and successfully applied to the study of percolation in MI composites [25,26]. Some interesting features of both one and two critical exponents versions of the GEM equation were discussed in a recent study [27]. It is important to mention that an important characteristic concerning the GEM equation is that it reduces to the classical percolation and effective medium equations when the appropriated limits are applied. Moreover, it is valid for composite materials comprised of phases with finite values of the electrical resistivity (conductivity) in the full range of composition, with any spatial distribution of phases [11]. The classical percolation theory, on the other hand, is valid only near the percolation threshold for a mixture of perfect conductors/insulators, and the effective media Bruggeman's equations (symmetric and asymmetric) require special spatial distribution of phases [11].

Within this context, the microstructural characterization and a careful analysis of the electrical conductivity dependence on the insulator volume fraction of YSZ-yttria composites are presented here. Thus, the main purpose of this work is to study the percolation in solid electrolyte (yttria-fully stabilized zirconia)-insulator (yttria) ceramic composites using the impedance spectroscopy technique and the GEM model.

2. Experimental

The starting oxides were ZrO_2:8 mol% Y_2O_3 (YSZ from Nissan, Japan) and yttrium oxide (Alpha Products). The metallic impurities content of the YSZ powder was determined by spectrographic analysis. Main impurities known to modify the electrical resistivity of zirconia like silicon and aluminum [28,29] were found in concentrations lower than the detection limit of the technique (60 ppm). Samples of (ZrO_2:8 mol% Y_2O_3) + m mol% Y_2O_3 with nominal yttria concentration m varying from 0 to 70 mol% (0–82.9 vol.%) were prepared by evaporation of a suspension of ZrO_2:8 mol% Y_2O_3 and Y_2O_3 in ethanol. The suspensions were homogenized in a mechanical mixer (Turbula T2C) for 3 h with 40 vol.% of ethanol followed by dispersion in ultrasound (Sonics and Materials) for 7 min. The evaporation was slowly carried out during mixing at 75 °C and the resulting powder was ground in an agate mortar.

Cylindrical pellets were prepared by uniaxial and isostatic pressing at 100 and 200 MPa, respectively; typical

final dimensions were about 2 mm thickness and 10 mm diameter. Sintering was carried out in alumina crucibles (with a zirconia powder bed) in a resistive furnace at 1350 °C for 0.1 h in air with a heating rate of 8 °C/min and furnace cooling. The short sintering time was used to avoid grain growth and the solubilization of yttria in the stabilized zirconia matrix.

The specimens were analyzed at room temperature by X-ray diffraction (Bruker-AXS D8 Advance), using Cu K_α radiation in the $10 \le 2\theta \le 90°$ range with a 0.02° (2θ) step size and 2 s counting time.

Polished and thermally etched surfaces were observed in scanning electron microscope (JEOL JSM5300) for morphology evaluation. Samples were polished with diamond paste; grain boundaries were revealed by thermal etching at 1250 °C for 30 min and surfaces were covered with gold by sputtering under argon. Average grain sizes were determined by the Mendelson method [30].

The electrical properties were determined by IS measurements from 300 to 500 °C in the 5 Hz–13 MHz frequency range with 100 mV signal amplitude, with a Hewlett Packard 4192A LF impedance analyzer connected to a HP 362 controller. Silver paste electrodes were applied to specimens and cured at 400 °C for 15 min. An inconel-600 sample chamber with type S thermocouple and platinum leads was used inside a resistive furnace for measuring three samples at the same temperature. One yttria-stabilized zirconia sample (previously measured) was kept in the sample chamber during all measurements to determine accurately the temperature. This procedure resulted in impedance measurements with a temperature control accuracy of 0.5 °C. All impedance diagrams were normalized to a geometrical factor equal to one.

3. Results and discussion

Fig. 1 shows the X-ray diffraction patterns of (ZrO_2:8 mol% Y_2O_3) + m mol% Y_2O_3 composites. All specimens show diffraction peaks corresponding to cubic zirconia. The diffraction peaks due to yttrium oxide are detected for nominal Y_2O_3 concentrations higher than 10 mol% and their relative intensities increase with yttria addition. No diffraction peaks corresponding to any reaction product of the oxides were detected.

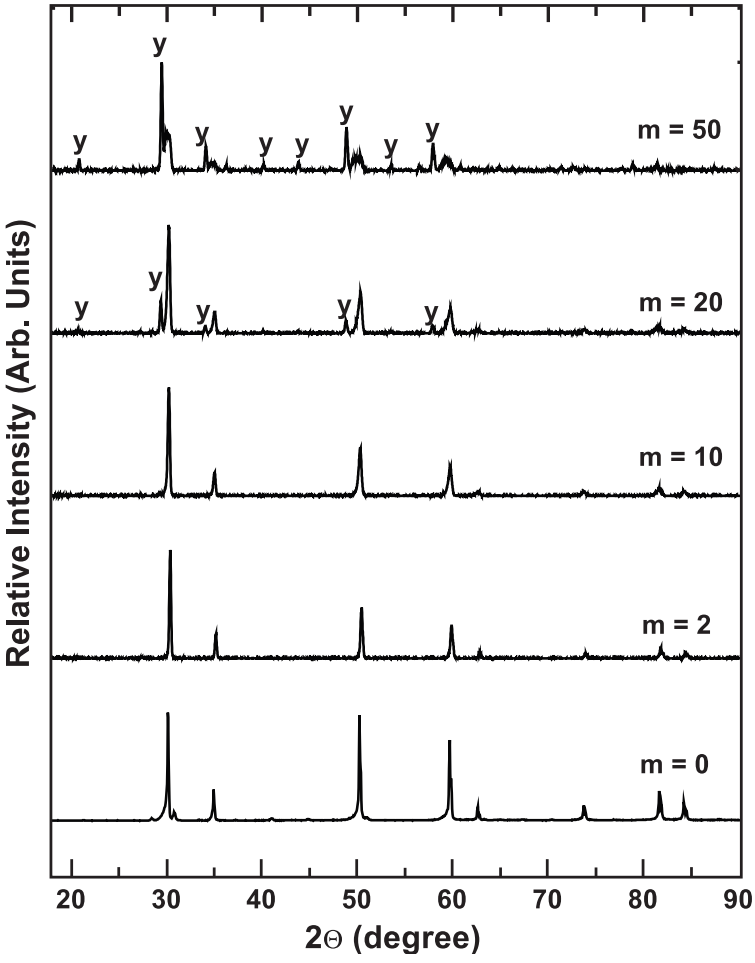

Fig. 1. X-ray diffraction patterns of (ZrO_2:8 mol% Y_2O_3) + m mol% Y_2O_3 for m = 0, 2, 10, 20 and 50; the main diffraction peaks of yttria are marked as "y".

The lattice parameter of cubic zirconia was determined for all compositions [31] and no dependence on the yttria content was observed. In fact, the average value (considering all the studied compositions) of the cubic zirconia lattice parameter is $a = 5.1321 \pm 0.0095$ Å, in good agreement with reported values for YSZ (ICDD file no. 30–1468). This result suggests that yttrium oxide is present as a second phase and no solid solution is formed since the substitution of Zr^{4+} ($r = 0.081$ nm) by Y^{3+} ($r = 0.090$ nm) is expected to increase the cubic zirconia lattice parameter.

Fig. 2 shows scanning electron microscopy (SEM) micrographs of (ZrO_2:8 mol% Y_2O_3) + m mol% Y_2O_3 for $m = 1$ (a) and 2 (b). It can be observed that the specimens with low yttria concentrations are dense with low intergranular porosity. The average grain size for both the samples $m = 1$ and 2 is 0.7 ± 0.3 μm. For higher yttria concentrations, the SEM analysis (not shown) indicates that the average grain size is reduced, suggesting that yttria as a second phase in YSZ acts as grain growth inhibitor in a manner similar to alumina and magnesia [29,32]. Also, for increasing yttria concentration, a decrease to ~ 80% of the theoretical density (TD) is observed (see Table 1). Microanalysis performed by energy dispersive spectra (not shown) revealed that yttria-rich regions can be found in specimens with low insulator content ($m = 2$ mol%), indicating that the solid solution was not attained even for low insulator concentrations.

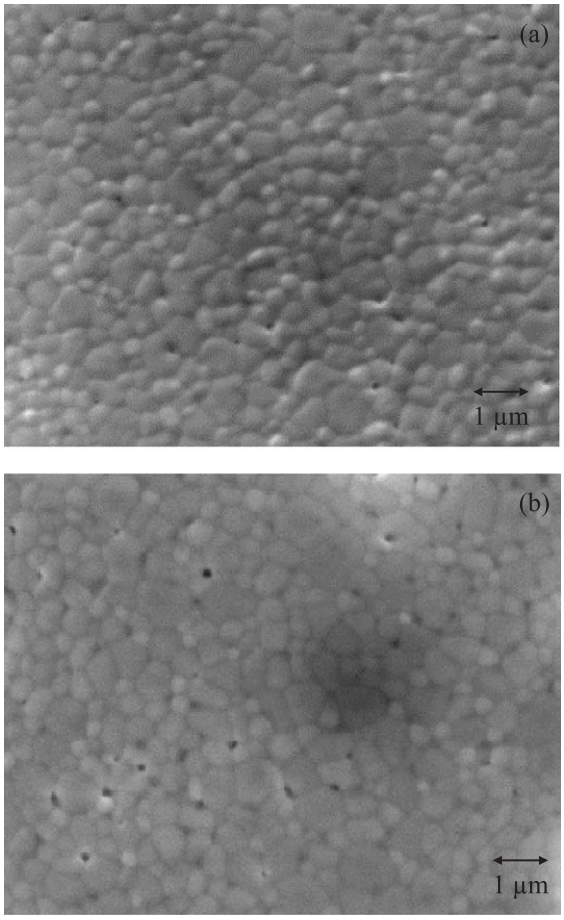

Fig. 2. Scanning electron microscopy micrographs of (ZrO_2:8 mol% Y_2O_3) + m mol% Y_2O_3 samples for $m = 1$ (a) and 2 (b).

Table 1
Yttria volume fraction and relative theoretical density (%TD) of the composite samples. The depression angles β of the fitted intergranular (LF) and intragranular (HF) components of the impedance diagrams and the respective activation energies calculated from the Arrhenius plots are also presented

Y_2O_3 (mol%)	Y_2O_3 (vol.%)	%TD*	β_{HF} (°)	β_{LF} (°)	ΔE_{HF} (eV)	ΔE_{LF} (eV)
0	0	95	9.5	10.1	1.1	1.1
1	2.05	97	7.6	11.1	1.1	1.1
5	9.81	92	8.0	14.7	1.1	1.2
10	18.69	95	11.7	15.7	1.0	1.3
20	34.13	83	14.1	17.2	0.9	1.2
30	47.02	78	–	15.5	–	1.3
50	67.44	78	–	12.1	–	1.3

* The composite densities were calculated after samples' geometrical dimensions and the theoretical values were determined by the rule of mixture using the reported values for YSZ (6.01 g/cm^3) and yttria (5.03 g/cm^3).

The main conclusions drawn from both XRD and SEM results are: (1) no reaction was detected within the resolution of XRD; (2) yttrium is dispersed as a second phase in cubic zirconia for concentrations between 2 and 70 mol%; (3) the average grain size decreases for increasing yttria content; and (4) the porosity increases for increasing yttria content. Both (3) and (4) results may represent, in principle, some difficulties to the percolation analysis and are discussed in detail.

We shall now concentrate on the electrical properties of the composite and their relation with the observed microstructural properties. The percolation analyses of the studied ionic conductor–insulator composite is expected to depend on the electrical properties of zirconia-based solid electrolytes. Thus, the effects of three important microstructural features on the electrical conductivity of YSZ are considered here.

(a) *The stabilizer content*

In this case, the 8 mol% yttria-stabilized zirconia has the optimized stabilizer content for a maximum electrical conductivity. It is known that higher added amounts of the stabilizer (>8 mol% for yttria) results in a decrease of the intragranular electrical conductivity of cubic zirconia electrolytes [33]. This decrease is usually ascribed to defect interactions [33]. In the present study, even if a small quantity of yttria (less than 2 mol%, as inferred by SEM analysis) solubilizes into stabilized zirconia, the expected decrease of the electrical conductivity should be approximately the same for all concentrations.

(b) *The average grain size*

The dependence of the grain boundary resistance on the average grain size has already been studied [34–37]. The

main conclusion is that the grain boundary electrical resistance decreases for increasing grain size, particularly for grain sizes larger than 1 μm. It was found that yttria addition reduces the YSZ grain size, mainly for high yttria concentrations ($m > 20$ mol%). However, the relative small initial grain sizes (< 1 μm) observed for specimens with $m < 20$ mol% should not be reduced more than one order of magnitude with increasing yttria content. In fact, such a reduced initial grain sizes values are smaller than the grain size range (~ 1 μm) where the larger variations of the electrical resistivity are observed due to decreasing grain size [37,38]. Thus, the electrical transport dependence on the grain size would be less pronounced in the studied specimens in comparison to a larger initial grain size. The lower limit case would be YSZ having grains in the nanometric scale, with a high density of grain boundaries. In this case, the intragranular response is almost independent and the intergranular response increases with decreasing grain size. For nanosized zirconia-based systems, the intergranular response was found to increase approximately six times in comparison to a micron-scale grain size [37,38]. Therefore, even though a reduction of grain size is observed, it does not fully explain the measured increase of the intergranular electrical resistance (close to four orders of magnitude) in the studied composite (see Fig. 5). Moreover, considering metal-insulator composites, if the average particle size of the metallic component decreases with increasing addition of the insulating phase, while the insulating particles keep the same size, it is expected that the percolation threshold will be reached at higher amounts of the insulator, in comparison to an ideal system where the particle size of both phases are independent on the relative volume fraction. Thus, the results of the percolation threshold obtained here should be considered as an upper limit of the actual value for the YSZ-yttria system.

(c) *The pore density*

In the present study, the percolation analysis accounts for a sum of both porosity and yttria blocking of charge carriers. Pores are supposed to contribute along with yttria blocking to the electrical resistivity, and both contributions are

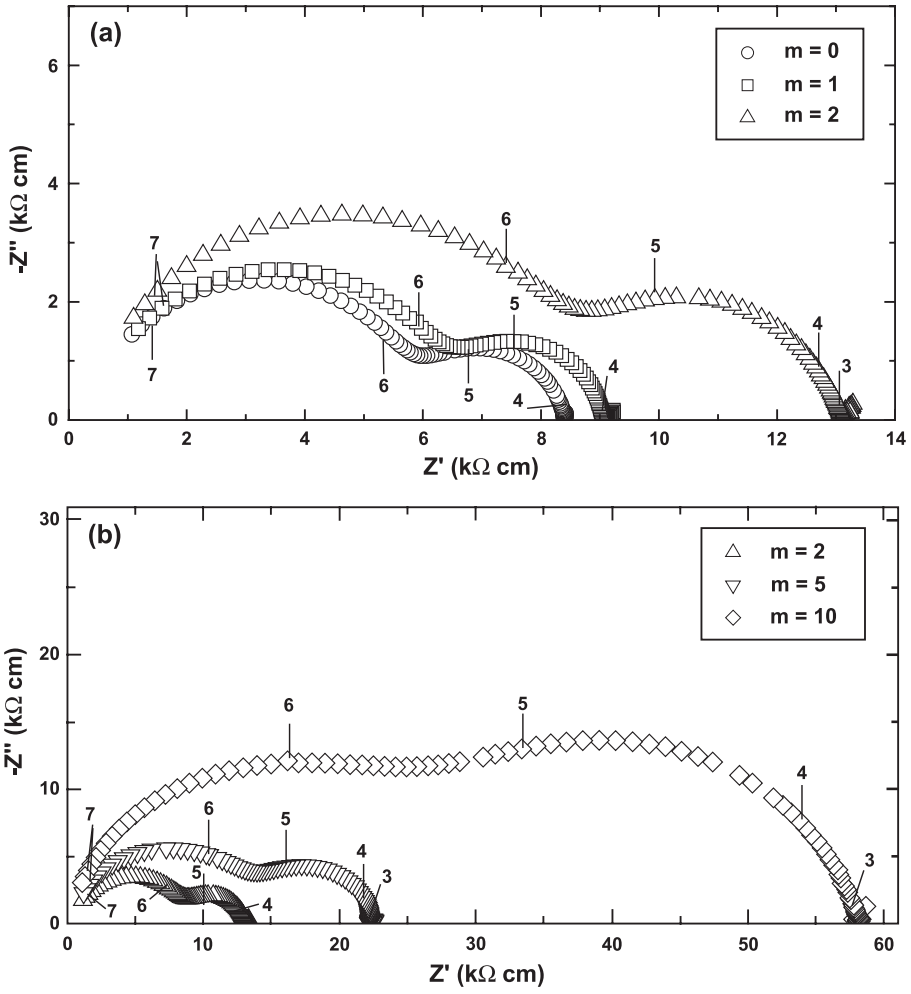

Fig. 3. Impedance diagrams of (ZrO_2:8 mol% Y_2O_3) + m mol% Y_2O_3 samples for $m = 0$, 1, 2 (a); $m = 2$, 5, 10 (b); $m = 10$, 12, 17, 20, 22, 25, 27 (c); and $m = 25$, 27, 30, 32, 40, 50, 60, 70 (d), measured at 390 °C. Numbers indicate the logarithm of frequency.

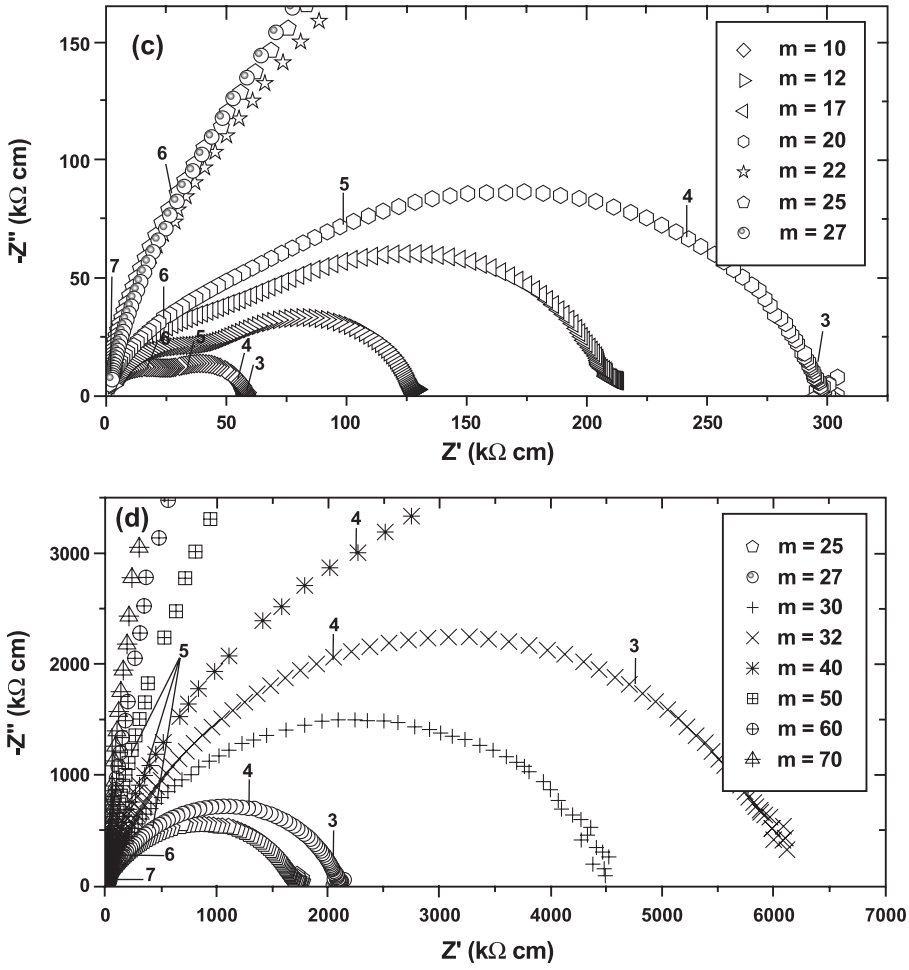

Fig. 3 (*continued*).

associated with the LF semicircle (intergranular) on the impedance diagrams (see Fig. 3). However, for yttria concentrations in which porosity is significant, $m > 20$ mol% (34.1 vol.%), the blocking of charge carriers (and the corresponding increase in the electrical resistivity) is expected to be much more influenced by the large insulator volume fraction than by porosity. Table 1 shows some typical values of the theoretical densities and the respective yttria volume fractions. It is possible to observe that, for $m < 20$ mol%, the studied samples have ~95% of the expected value of the dense composite. Increasing yttria content results in a decrease of the relative TD to ~ 80%, and this value seems to be nearly independent on the yttria content for higher concentrations. It was already reported for YSZ electrolytes that the electrical resistivity increases approximately four times for specimens having 97% and 77% of the TD [8]. Indeed, samples with $m \geq 20$ mol% have comparable relative theoretical densities, but very different electrical conductivities, which is attributed to the high volume fractions of the insulating yttrium oxide (see Figs. 3–5). Therefore, it can be considered that the pronounced decrease of the electrical conductivity with yttria addition is mainly related to the insulating phase content rather than to porosity.

3.1. Impedance spectroscopy data analysis

The IS diagrams of (ZrO_2:8 mol% Y_2O_3) + m mol% Y_2O_3 measured at 390 °C are shown in Fig. 3. Samples with concentrations up to $m = 20$ mol% (34.1 vol.%) (Figs. 3a–c) show two well-defined semicircles, one at HF related to cubic stabilized zirconia intragranular (bulk) properties, and another at LF related to the blocking of charge carriers caused by the added insulating phase and to grain boundaries [3]. IS diagrams of samples with yttria content $m = 25$ and 27 mol% were resolved using a two semicircles model to account for high frequency deviations from a model with only one arc. For yttria concentrations $m > 30$ mol% (47.0 vol.%) (Fig. 3d), only one semicircle is observed and the specimens have values of the total electrical resistivity of the order of 10 MW cm. The increase of the electrical resistivity is attributed to the blocking of oxide ions by the insulating phase and the high values of the electrical resistivity observed for high insulator volume fraction ($m \geq 30$ mol%

or 47.0 vol.%) may be responsible for the complete overlapping of the HF semicircle due to the dominant LF contribution. The impedance diagrams are similar to those obtained for stabilized zirconia with alumina addition [4]: with increasing insulating phase addition the low frequency semicircles have a larger increase than the high frequency semicircles. Thus, the increase in the LF semicircle is a further evidence that yttria is dispersed as a second insulating phase. Considering the evolution of the IS data with increasing insulator addition, the only arc observed for $m \geq 30$ mol% is a sum of both HF and LF contributions, strongly dominated by the LF component, and then it was associated with this contribution. Consequently, the HF component could only be resolved over a limited range of insulator content ($m < 30$ mol%).

The impedance diagrams were fitted using an equivalent circuit model (two parallel RC circuits connected in series) to obtain the electrical conductivity σ (the reciprocal of the semicircle arc diameter), characteristic frequency ω_0 (apex frequency of a semicircle arc) and the decentralization angle β (the depression of a semicircle from the real axis). As displayed in Table 1, typical values for the HF semicircle are $\beta_{HF} \sim 10°$ and for the LF component the β_{LF} values are a little higher, as expected, in the 10–20° range. These β values seem to increase with increasing addition of the insulating phase, which is probably associated with the higher degree of heterogeneity of the samples with increasing yttria content [8].

The transport properties of the composite were also investigated by the Arrhenius plots of the electrical conductivity, as shown in Fig. 4. The HF and LF electrical conductivity components determined from the fittings of the impedance diagrams measured at several temperatures were used to calculate the thermal activation energies ΔE from the Arrhenius plots, according to the expression:

$$\sigma = \frac{\sigma_0}{T} . exp\left(-\frac{\Delta E}{kT}\right) \quad (2)$$

where σ_0 is the temperature independent electrical conductivity, ΔE the activation energy, k the Boltzmann constant and T the absolute temperature. All samples exhibit a thermally activated behavior of the total, intragranular and intergranular electrical conductivities with $\Delta E \sim 1$ eV, which is the value usually found for zirconia-based solid electrolytes [39], indicating that the basic charge transport is not modified in the composition range studied (see Table 1). Slightly higher (~ 10%) values of the intergranular ΔE_{LF} were obtained, in good agreement with previously reported values [4]. These results indicate that the oxide ion electrical conduction mechanism is not significantly changed with the insulator addition. The main difference found in the Arrhenius plots for the different compositions of the insulating phase is the decrease of σ_0 for increasing yttria content. This is associated with the decreasing mobility of charge carriers with increasing yttria addition, since there is no appreciable change of the number of charge carriers in these composites.

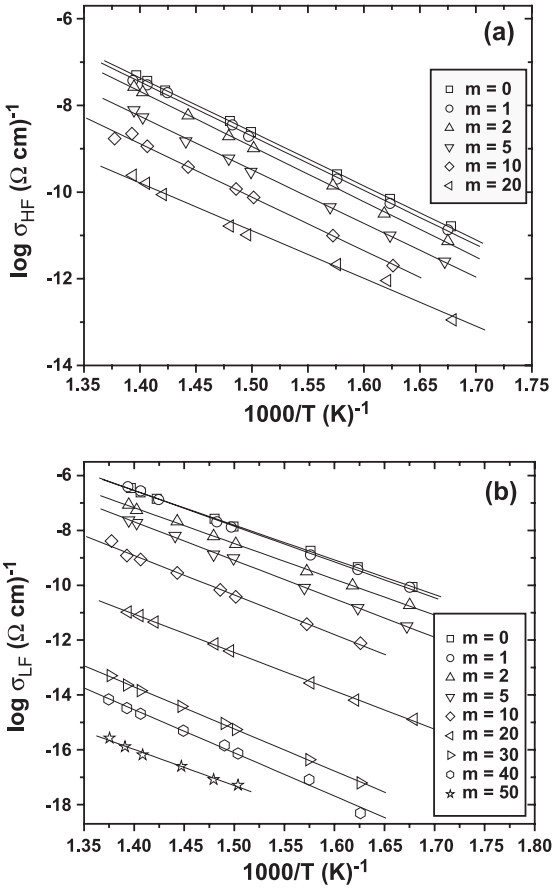

Fig. 4. Arrhenius plots of the intragranular (a) and intergranular (b) conductivities of (ZrO_2:8 mol% Y_2O_3) + m mol% Y_2O_3 for m = 0, 1, 2, 5, 10, 20, 30, 40 and 50. The linear best fittings are also shown.

A four orders of magnitude decrease of the total and intergranular electrical conductivities is observed for increasing Y_2O_3 content in relation to the YSZ pristine sample. The dependence of the electrical conductivity components on the insulator content is that of a conductor–insulator composite, being the blocking by yttria the major responsible for the decrease in the total electrical conductivity. The pronounced decrease of the electrical conductivity as a function of insulator phase content suggests that the composite has undergone a percolative transition, with a percolation threshold at a critical volume fraction (f_C) between 20 and 30 mol% (34.1 and 47 vol.%). The normalized values of the total (a), intragranular (b) and intergranular (c) electrical conductivities of (ZrO_2:8 mol% Y_2O_3) + m mol% Y_2O_3 measured at 390 °C as a function of yttria volume fraction and the fitted GEM equation (Eq. (1)) are shown in Fig. 5.

The GEM equation fitting to the experimental data was performed minimizing the parameter δ given by [20,21]:

$$\delta = [\chi^2/(N-P)]^{1/2} \quad (3)$$

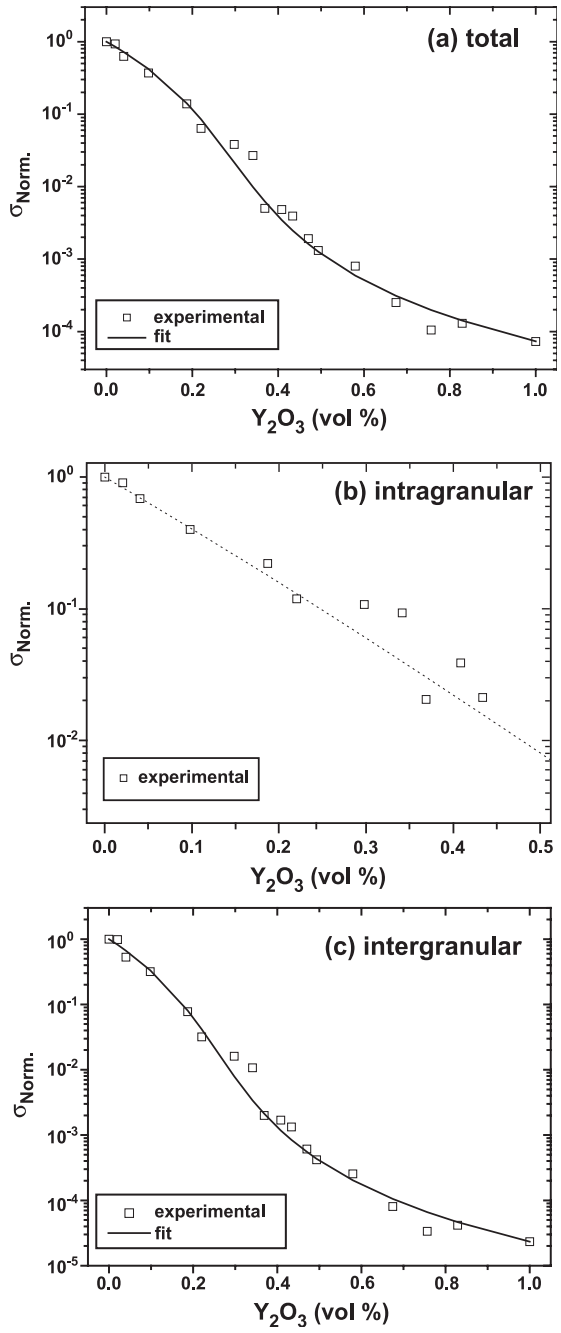

Fig. 5. Total (a), intra- (b) and intergranular (c) electrical conductivity of (ZrO_2:8 mol% Y_2O_3)+m mol% Y_2O_3 as a function of Y_2O_3 volume fraction. The general effective medium equation fitting for the total and intergranular components are also shown. All electrical conductivity values, measured at 390 °C, were normalized to the electrical conductivity of cubic zirconia.

where N is the number of experimental points, P the number of variable parameters and χ is given by:

$$\chi^2 = \sum_N [(\sigma_{Fit} - \sigma_{Exp})/\lambda_{Exp}]^2 \quad (4)$$

where σ_{Fit} was obtained by GEM equation (Eq. (1)) using the nominal yttria volume fraction and the electrical conductivities of cubic zirconia and yttria [40], σ_{Exp} was obtained by IS measurements and λ_{Exp} was assumed as 10% of the electrical conductivity experimental values [20,21].

A good agreement between the experimental data and the GEM equation is observed in Fig. 5. Similar results were obtained at other measuring temperatures close to 400 °C, lending credence to our analysis. The observed decrease of the intragranular electrical conductivity (Fig. 5b) is similar to the already reported decrease of the intragranular conductivity of stabilized zirconia with controlled additions of blockers, like alumina and pores [4]. Moreover, it is a percolative process related to the decrease of the volume fraction of cubic zirconia grains [4,32]. However, due to a reduced number of experimental data, the determined critical volume fraction value f_{CHF} for this contribution lacks of statistical significance. The percolation thresholds of the total and intergranular components (Fig. 5a and c) were found to be $f_{CT} = 30 \pm 1$ vol.% and $f_{CLF} = 27 \pm 1$ vol.%, respectively. In the present study, the main reason for such relatively high f_C values is possibly related to the grain size and porosity dependencies on the insulator content [11,19]. These values indicate that the percolation threshold for the total electrical conductivity occurs at higher (~ 10%) concentrations in relation to the intergranular conductivity. This could be associated with the intrinsic blocking of charge carriers at internal surfaces (mainly non-conducting grain boundary regions) of zirconia-based solid electrolytes.

The critical exponent t values determined for the total and LF contributions are ~ 2.5. Although the t values for the total and intergranular component are not far from the universality range [11,19], a more detailed discussion regarding the critical exponent needs further considerations that are beyond the scope of the present study [25].

In summary, the main results show that impedance spectroscopy is an important technique for the evaluation of the actual contributions to percolation, especially for materials with a partial intrinsic blocking of charge carriers. The separation of the different contributions in the frequency domain permitted by the impedance spectroscopy technique can be also useful to study percolation phenomena on composite materials with porous matrices or more than two phases, provided their contributions to the electrical transport differ, allowing for the deconvolution of the impedance diagrams. The study of the different contributions to the electrical conductivity can be very important on the design of specific composite materials for applications with well-controlled functional electrical properties.

4. Conclusions

The electrical conductivity of the solid electrolyte (ZrO_2:8 mol% Y_2O_3)-insulator (Y_2O_3) composite system was studied by impedance spectroscopy. The dependence of the intragranular and intergranular contributions to the electrical conductivity upon the insulator content was analyzed according to the general effective medium equation

resulting in good agreement with the experimental data. The percolation thresholds for the total and intergranular contributions were 30 and 27 vol.%, respectively. Considering the observed dependence on the insulator content of both average grain size and porosity, the obtained critical volume fractions may be regarded as an upper limit for the studied composite. In addition, the results indicate that impedance spectroscopy can provide more detailed information about percolation parameters (critical volume fraction and critical exponent) than dc techniques, for systems that exhibit a partial blocking of charge carriers such as stabilized zirconia solid electrolytes.

Acknowledgements

We would like to thank CNEN, FAPESP (97/00727-3, 98/14324-0 and 99/10798-0), CNPq (306496/88-7) and PRONEX for financial support and scholarships. Thanks are also due to Dr. M.C. Steil (LCPS, ENSC, Lille, France) for SEM analyses.

References

[1] A. Bieberle, L.P. Meier, L.J. Gaucklser, J. Electrochem. Soc. 148 (2001) A646.
[2] M.J. Jorgensen, M. Mogensen, J. Electrochem. Soc. 148 (2001) A433.
[3] J. Bauerle, J. Phys. Chem. Solids 30 (1969) 2657.
[4] M. Kleitz, L. Dessemond, M.C. Steil, Solid State Ionics 75 (1995) 107.
[5] M. Kleitz, M.C. Steil, J. Eur. Ceram. Soc. 17 (1997) 819.
[6] M. Kleitz, L. Dessemond, M.C. Steil, F. Thevenot, in: R.A. Gerhardt, S.R. Taylor, E.J. Garboczi (Eds.), Mat. Res. Symp. Proc., vol. 411 1996, pp. 269.
[7] M.C. Steil, F. Thévenot, L. Dessemond, M. Kleitz, Third Euro-Ceramics (Madrid, Spain) 2 (1993) 271.
[8] M.C. Steil, F. Thévenot, M. Kleitz, J. Electrochem. Soc. 144 (1997) 390.
[9] N.F. Uvarov, Solid State Ionics 136 (2000) 1267.
[10] C.M. Mari, G. Dotelli, J. Math. Sci. 36 (2001) 1141.
[11] D.S. McLachlan, M. Blaszkiewicz, R.E. Newnham, J. Am. Ceram. Soc. 73 (1990) 2187.
[12] C.C. Liang, J. Electrochem. Soc. 120 (1973) 1289.
[13] P. Knauth, J.-M. Debierre, G. Albinet, Solid State Ionics 121 (1999) 101.
[14] J. Maier, Prog. Solid State Chem. 23 (1995) 171.
[15] A. Bunde, W. Dieterich, H.E. Roman, Phys. Rev. Lett. 55 (1985) 5.
[16] D. Stauffer, Phys. Rep. 54 (1979) 1.
[17] D.M. Grannan, J.C. Garland, D.B. Tanner, Phys. Rev. Lett. 46 (1981) 375.
[18] Y. Song, T. Won, S.-I. Lee, J.R. Gaines, Phys. Rev. B33 (1986) 904.
[19] D.S. McLachlan, J. Electroceramics 5 (2000) 93.
[20] D.S. McLachlan, J. Phys. C. Solid State Phys. 21 (1988) 1521.
[21] D.S. McLachlan, Jpn. J. Appl. Phys. 26 (Suppl. 3) (1987) 901.
[22] F.C. Fonseca, R. Muccillo, Phisica C 267 (1996) 87.
[23] V.Y. Petrovsky, Z.S. Rak, J. Eur. Ceram. Soc. 21 (2001) 237.
[24] F.M. Figueiredo, F.M.B. Marques, J.R. Frade, Solid State Ionics 138 (2001) 173.
[25] J. Wu, D.S. McLachlan, Phys. Rev. B 56 (1997) 1236.
[26] D.S. McLachlan, K.F. Cai, G. Sauti, Int. J. Refract. Met. H 19 (2001) 437.
[27] J. Runyan, R.A. Gerhardt, R. Ruh, J. Am. Ceram. Soc. 84 (2001) 1490.
[28] E.P. Butler, R.K. Slotwinski, N. Bonanos, J. Drennan, B.C.H. Steele, Science and technology of Zirconia II, in: N. Claussen, M. Rühle, A.H. Heuer (Eds.), Advances in Ceramics, vol. 12, The American Ceramic Society, Columbus, Ohio, USA, 1983, pp. 572–584.
[29] S. Rajendran, J. Drennan, S.P.S. Badwal, J. Mater. Sci. Lett. 6 (1987) 1431.
[30] M.I. Mendelson, J. Am. Ceram. Soc. 52 (1969) 443.
[31] R.P. Ingel, D. Lewis III, J. Am. Ceram. Soc. 69 (1986) 325.
[32] F.C. Fonseca, R. Muccillo, Solid State Ionics 131 (2000) 301.
[33] J.F. Baumard, P. Abelard, Science and technology of Zirconia II, in: N. Claussen, M. Rühle, A.H. Heuer (Eds.), Advances in Ceramics, vol. 12, The American Ceramic Society, Columbus, Ohio, USA, 1983, pp. 555–571.
[34] A.I. Ioffe, M.V. Inozemtzev, A.S. Lipilin, M.V. Perfilev, S.V. Karpachov, Phys. Status Solidi A 30 (1975) 87.
[35] S.H. Chu, M.A. Seitz, J. Solid State Chem. 23 (1978) 287.
[36] M.J. Verkerk, B.J. Middelhuis, A.J. Burggraaf, Solid State Ionics 6 (1982).
[37] X. Guo, Z. Zhang, Acta Mater. 51 (2003) 2539.
[38] H.L. Tuller, Solid State Ionics 131 (2000) 143.
[39] F.T. Ciacchi, K.M. Crane, S.P.S. Badwal, Solid State Ionics 73 (1994) 49.
[40] A.F. Andreeva, A.G. Sisonyuk, E.G. Himich, Phys. Status Solidi A 145 (1994) 441.